



HAL
open science

Simplified modelling of the behaviour of 3D-periodic structures such as aircraft heat exchangers

Jihad Rishmany, Catherine Mabru, Rémy Chieragatti, Farhad Rezai-Aria

► **To cite this version:**

Jihad Rishmany, Catherine Mabru, Rémy Chieragatti, Farhad Rezai-Aria. Simplified modelling of the behaviour of 3D-periodic structures such as aircraft heat exchangers. *International Journal of Mechanical Sciences*, 2008, 5 (6), pp.1114-1122. 10.1016/j.ijmecsci.2008.01.006 . hal-01691599

HAL Id: hal-01691599

<https://hal.science/hal-01691599>

Submitted on 24 Jan 2018

HAL is a multi-disciplinary open access archive for the deposit and dissemination of scientific research documents, whether they are published or not. The documents may come from teaching and research institutions in France or abroad, or from public or private research centers.

L'archive ouverte pluridisciplinaire **HAL**, est destinée au dépôt et à la diffusion de documents scientifiques de niveau recherche, publiés ou non, émanant des établissements d'enseignement et de recherche français ou étrangers, des laboratoires publics ou privés.



Open Archive TOULOUSE Archive Ouverte (OATAO)

OATAO is an open access repository that collects the work of Toulouse researchers and makes it freely available over the web where possible.

This is an author-deposited version published in : <http://oatao.univ-toulouse.fr/>
Eprints ID : 239

To link to this article : DOI: 10.1016/j.ijmecsci.2008.01.006
URL : <http://dx.doi.org/10.1016/j.ijmecsci.2008.01.006>

To cite this version : Rishmany, Jihad and Mabru, Catherine and Chieragatti, Rémy and Rezaï-Aria, Farhad *Simplified modelling of the behaviour of 3D-periodic structures such as aircraft heat exchangers*. (2008) International Journal of Mechanical Sciences, vol. 5 (n° 6). pp. 1114-1122. ISSN 0020-7403

Any correspondence concerning this service should be sent to the repository administrator: staff-oatao@listes-diff.inp-toulouse.fr

Simplified modelling of the behaviour of 3D-periodic structures such as aircraft heat exchangers

J. Rishmany, C. Mabru*, R. Chieragatti, F. Rezaï Aria^a

*Ecole Nationale Supérieure d'Ingénieurs de Constructions Aéronautiques
1, Place Emile Blouin, 31056 Toulouse, France*

*^aEcole des Mines d'Albi-Carmaux
Route de Teillet, 81013 Albi, France*

* Corresponding author: catherine.mabru@ensica.fr

Abstract

In this paper, experimental, analytical and numerical analysis are used to study and model the mechanical behaviour of a heat exchanger core consisting of a 3D-periodic structure. The purpose of the present investigation is not only to acquire knowledge on the mechanical behaviour of a given heat exchanger core but also to propose a simplified approach to model this behaviour. An experimental study is carried out in order to get an insight on the mechanical behaviour of this structure. Global static characteristics are obtained via analytical and finite element analysis of a unit cell of the core. Dynamic behaviour is studied by means of finite element calculations based on the results of the static modelling. The proposed approach is validated by comparison with experimental tests results.

Keywords: aircraft heat exchanger; periodic structure; finite element method.

1. Introduction

Aircraft heat exchangers are subjected in service to a complex loading combining pressure, temperature and vibration. Due to this complex loading, the prediction of the lifetime of exchangers is extremely

difficult. Testing of such equipments under real service conditions is also very expensive and time-consuming. An alternative solution is therefore to perform accelerated tests. However, this solution requires a prior understanding of the static and dynamic behaviour of the different parts of the exchanger, and in particular, of the core behaviour. This last point constitutes the subject of this study. Each part of the exchanger is designed apart according to specific criteria. For example, mechanical resistance is considered to dimension the inlet and outlet air stream ports as well as their attaching device whereas both heat transfer and fluid mechanics are mainly considered to dimension the exchanger core. The mechanical analysis of the core is done separately on its components (fins and parting sheets) considering the working pressure. However, the global mechanical behaviour of the exchanger core is currently extremely simplified due to its complex 3D structure and the subsequent difficulty to model it. On one hand, analytical solutions are difficult to obtain and, on the other hand, using classical finite elements methods would lead to several millions of elements and thus can not be considered as a valuable approach. In addition, public literature on the global mechanical behaviour of such aircraft heat exchanger cores is very poor.

The purpose of the present investigation is therefore not only to acquire knowledge on the mechanical behaviour of a given heat exchanger core but also to propose an approach to model this behaviour in a simplified manner. The obtained model could then be used in the modelling of the whole exchanger and/or with a wider range of loading, including thermal loading.

The equipment presently investigated is the core of an air-to-air compact heat exchanger. It consists of a block of alternating layers of fins separated by parting sheets and constitutes a 3D-periodic structure (Fig. 1). Several models addressing the mechanical behaviour of such structures are reported in literature. Models based on the classical laminate theory (CLT) [1-3] are widely used for wavy structures. However, these models present shortcoming for predictions of transverse moduli, E_{33} , and

G_{13} . Therefore, all the stiffness matrix elements of the core cannot be calculated by this approach, and thus no finite element calculations would further be possible to assess the dynamic behaviour of the core. Numerous methods based on homogenization or Representative Volume Element techniques (mean or periodic, asymptotic...) [4-8] used for heterogeneous materials could be extended to this structure problem [9-10]. However, these techniques demand specific numerical tools and tedious modelling. Subsequently they cannot answer to the request of simplicity of the present modelling. Nevertheless, the concept of isolating substructures behaviour to assess the global behaviour will be used in the present investigation.

The first part of this paper presents the experimental study carried out in order to get an insight on the mechanical behaviour of this structure and to obtain results that would further be used to validate the proposed modelling. The second part deals with the modelling of static behaviour, presenting analytical and numerical (finite element) approaches, both based on the study of a unit cell whose behaviour is supposed to be representative of the whole core. In the last part, the so-obtained equivalent stiffness matrix is used in a finite element dynamic analysis. The global behaviour of tensile and dynamic laboratory experiments is compared with the results of the model.

2. Core structure

The structure presently investigated is the core of an air-to-air compact aircraft heat exchanger. As mentioned earlier, the core of this heat exchanger consists of a block of alternating layers of fins. Fig. 1 shows a sketch presentation of the core. The layers are separated from each other by parting sheets and sealed along the edges by means of closure bars. They are provided with inlet and outlet ports for the passage of cold and hot air streams. End sheets at the top and bottom bound the block. The stacked assembly is brazed in a vacuum furnace to grant the rigidity of the core. The core constitutes a periodic

structure consisting of two alternative 0 and 90 ° plies. Each ply is set-up of fins that are bounded by two half-plates, thus forming a 3D-wavy-sandwich structure.

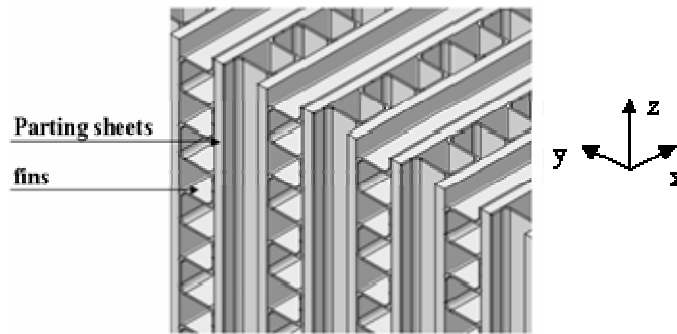


Fig. 1. A schematic presentation of the periodic structure of the heat exchanger core

The sheets and the fins are made of two isotropic materials with similar mechanical properties: E , the Young's modulus, ν , the Poisson's ratio, and G , the shear modulus.

Moreover, like sandwich structures, the core is supposed to have an orthotropic behaviour. Poisson's ratios are also neglected. The numerical FEM calculations have shown that such assumption is relevant.

3. Experimental study

3.1. Experimental procedures and specimen preparation

Tensile tests were conducted along two directions (y) and (z) on samples cut out from the core by electro-erosion. Specimens along (y) axis had either 7 hot passages and 8 cold passages (Fig. 2-b) or 15 hot passages and 16 cold passages in length. Their section contained 12 and 10 unit cells along (x) and (z) axis respectively. Specimens along (z) axis had a useful length containing 40 unit cells and a section containing 12 unit cells along (x) axis and 1 hot and 1 cold passages along (y) axis (Fig. 2-a). Tests along x -axis were not performed as it was supposed that if the model is validated for z -axis, it would be relevant for x -axis due to the similarity in the built up of the structure along these two directions. For tensile tests along z -axis, the two ends of the specimens were filled with resin to better distribute the

clamping forces and to limit stress concentrations. Reinforcing plates were also glued at both ends (Fig. 2-a, post-experiment photo) using a bi-component adhesive. Two extensometers were attached on the specimens for displacement measurement. For tensile tests along y-axis, shoulders were glued on both ends of the specimens (Fig. 2-b). One or more extensometers were attached on the specimens according to their length. Tensile to rupture tests were conducted at room temperature with a displacement rate of 0.5 mm/min according to two loading conditions: i) Continuous loading, ii) Several loading/unloading.



Fig. 2 . Tensile test samples along (a) z-axis (b) y-axis

For dynamic testing, samples similar to those used in tensile tests were employed. The impulse-response (IR) technique was applied. It is a non-destructive sonic method generally used to determine the dynamic properties (frequencies, damping ratios and mode shapes) of structural systems. The technique consists principally of two stages; striking the specimen with a mechanical device such as a hammer and then monitoring the response by attaching a transducer to the specimen. The impact force produced by the mechanical device during a short transient period induces stress waves, which reflect back and forth within the structural system between boundary interfaces until the mechanically induced energy is consumed by material damping, dispersion and reflections. For our experiments, the samples were hung freely using rubber elastics. A piezo-electric accelerometer was attached to the specimen using wax to measure the sample acceleration. An instrumented hammer, equipped with a force transducer to capture the induced force, was used to strike the specimen (Fig. 3). Signals from the instrumented hammer and accelerometer were fed into a 2-channel frequency analyzer with a high signal storage capability. For

each specimen, several striking tests were performed after changing the place of the accelerometer on the sample. Results were then post-treated using Matlab. Fast Fourier Transforms (FFT) of specimen responses were obtained from signal vs. time graphs. Numerous spectral peaks, which correspond to the resonance frequencies of the specimen, can be readily identified.

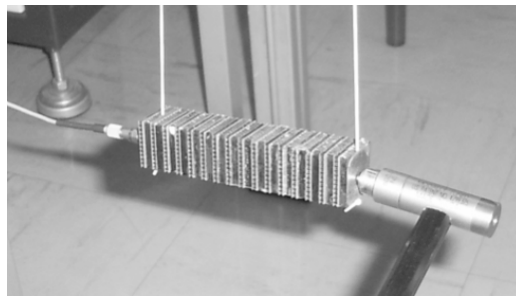


Fig. 3. Dynamic testing of specimen using IR technique

3.2. Experimental results

3.2.1 Tensile tests

Force-Deformation diagrams are reported for tensile tests in Fig. 4. For z-axis tests samples (Fig. 4-a), the curves are similar to what could be obtained by tensile tests on classical monolithic metallic specimens.

For y-axis tests specimens (Fig. 4-b) three different parts can be identified on the force-deformation curve:

- The first part presents a mean force-deformation slope (K_1) that is variable and sample dependant. It is assumed that the variable slope depends on the initial form of fins and corresponds to their unfolding at an early stage of the test.
- The second part presents a similar slope for all samples that represents the apparent elastic stiffness (K_2) of the tested structure.

- The third part describes the plastic behaviour of samples. The higher stiffness (K_3) noted in this last part during unloading is attributed to a structural effect combined with localized plasticity. This phenomenon has already been observed for cellular solids [11].

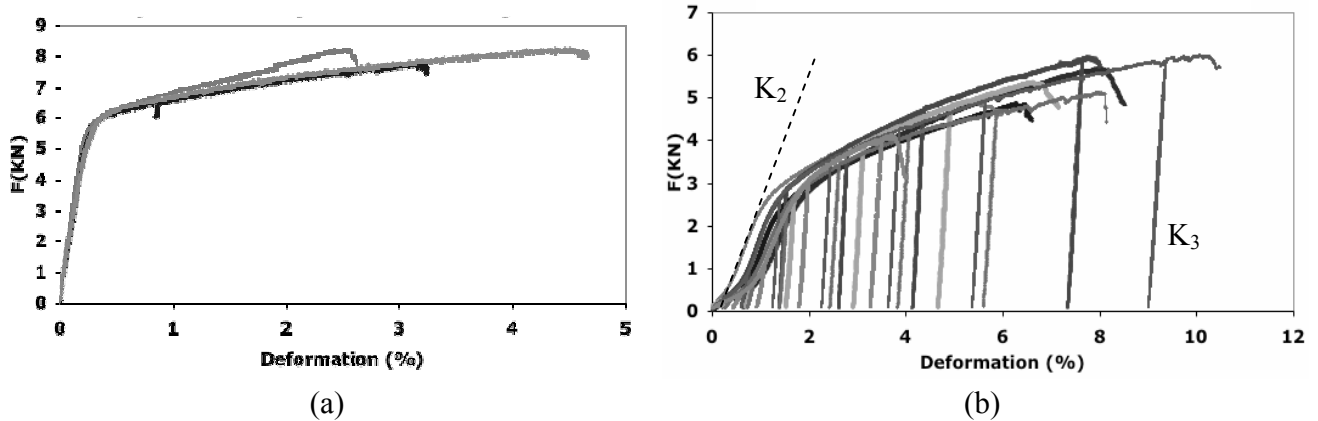


Fig. 4. Force-Deformation diagrams of tensile tests (a) z-axis (b) y-axis

Considering the loading experienced by the core during services and previous proof tests, the apparent stiffness (K_2) is assumed to be representative of the mechanical behaviour of the core in its normal use conditions.

3.2.2. Impulse-response tests

Impulse-response tests were performed on different samples having as longitudinal direction either the y-axis or the z-axis (similar to tensile test samples of Fig. 2). As an example, the Fourier Transform of a once struck y-axis sample response is plotted in Fig. 5. Exploited results are the values of the frequencies where the peaks are observed and corresponding to the resonance frequencies. Damping is not identified. In order to obtain the complete dynamic response of the sample, it is then necessary to carry out the same analysis for different striking, changing each time the position of the accelerometer. Dynamic response of samples is not representative of the dynamic behaviour of the complete structure; therefore the obtained results are only exploited to validate the proposed models and will be presented in section 5.2 for discussion.

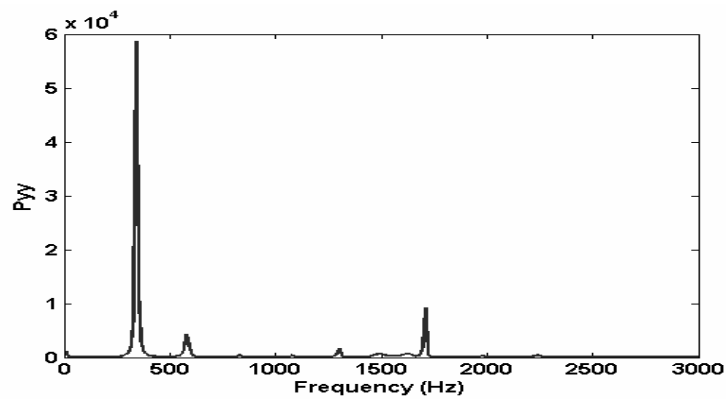


Fig. 5. Example of a Fourier Transform of y-axis sample response

4. Modelling of static behaviour

The main purpose of this part is to propose a method to determine an equivalent stiffness matrix for the heat exchanger core. Due to the size and the complexity of the core shown in Fig. 1, it is clear that a unique model representing the whole structure would be cumbersome and unwieldy. Therefore, a unit cell of the core is first studied by an analytical and numerical (Finite Element Modelling) approach. It is assumed that the behaviour of this unit cell is representative of the behaviour of the core. The so obtained average local stiffness of the unit cell is then used to estimate equivalent elastic modulus of the core. Fig. 6 presents the unit cell that has been chosen. It consists of two alternating fins separated by a sheet and bounded at the top and the bottom by two half-sheets. The 3D-structure of the core can be obtained by assembling several unit cells in all three directions.

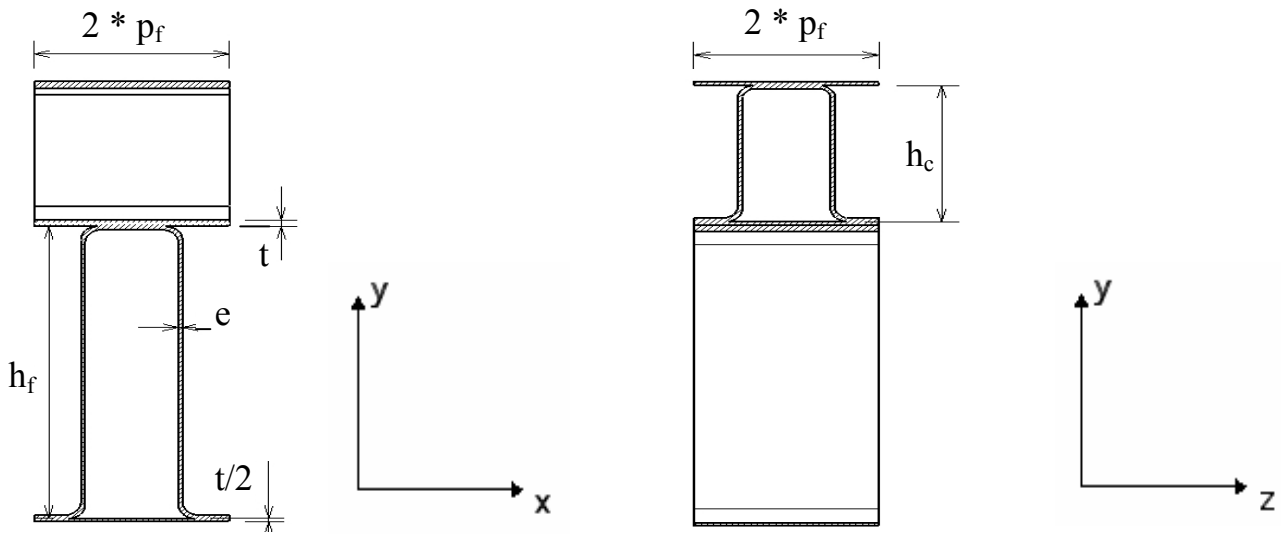


Fig. 6. Unit cell of the core

4.1. Analytical study

Formulation of equivalent tensile elastic moduli

The average stiffness of the unit cell is found by dividing it into (n) substructures, each having a stiffness (k_i) and replacing the unit cell by a spring network [12]. Hence, the estimation of the stiffness of the unit cell is reduced to calculate the equivalent stiffness of the spring network.

Moreover, in order to simplify the calculations, the following assumptions are made:

- Brazing and its effect on local stiffness and behaviour are neglected,
- The material has a linear-elastic behaviour,
- Perfect bonding exists between the fins and the sheets,
- Along (x) and (z) directions, deformation of the unit cell is mainly governed by the deformation of the plates and the longitudinal fins. Hence the stiffness of transversal fins is neglected along these two directions.

- Along (y) directions, beam theory is used on each layer to estimate separately the stiffness of cold air layer and hot air layer. Each layer is constructed with three basic plate/beam elements presented in Fig. 7.

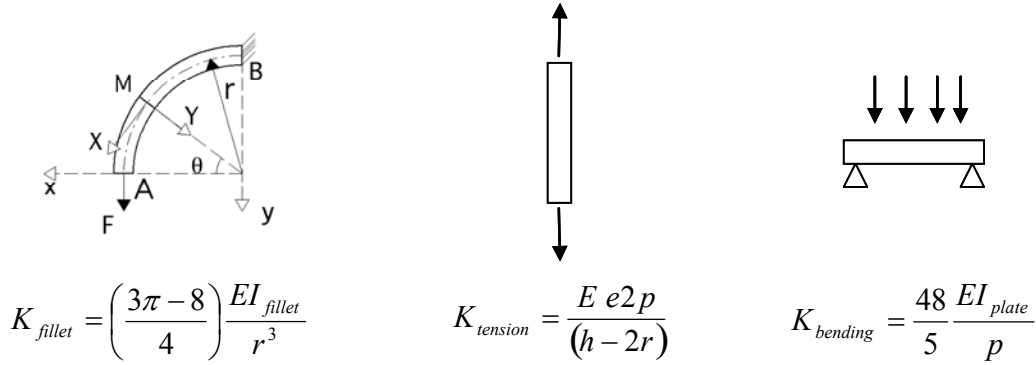


Fig. 7. Substructures and their corresponding analytical stiffness used for the estimation of the stiffness K_y of a unit cell

Equations (1), (2) and (3) give the analytical stiffness of the unit cell along (x), (z) and (y) axis respectively.

$$K_x = \frac{E(2tp_c + eh_c + ep_c)}{p_f} \quad (1)$$

$$K_z = \frac{E(2tp_f + eh_f + ep_f)}{p_c} \quad (2)$$

$$\frac{1}{K_y} = \left(\frac{2}{2K_{fillet}} + \frac{1}{2K_{tension}} + \frac{1}{K_{bending}} \right)_{cold\ layer} + \left(\frac{2}{2K_{fillet}} + \frac{1}{2K_{tension}} + \frac{1}{K_{bending}} \right)_{hot\ layer} \quad (3)$$

Once the stiffness of a unit cell is calculated, equivalent elastic modulus $E_{x,eq}$ (identical for the unit cell and for the whole core according to our hypothesis) can be estimated easily using equation (4).

$$E_{x,eq} = \frac{K_x l_x}{S_{x,eq}} \quad (4)$$

where K_x , l_x , and $S_{x,eq}$ are respectively the average stiffness, the length and the equivalent surface of the unit cell having as normal the x-axis.

The equivalent elastic moduli along (y) and (z) axes are found in a similar manner.

Formulation of equivalent core shear moduli G_{xz}^e and G_{yz}^e

Unlike the cases of tensile elastic moduli, the estimation of the shear moduli usually requires to consider a complicated state of deformation. It is then relatively difficult to get an exact analytical solution. However, the lower and upper bound solutions can be obtained by considering an energy-based approach [3]. The energy theory states that the strain energy calculated from the exact displacement distribution is a minimum. For a given structure, elastic energy can be generally expressed in parallel and series models according to Voigt and Reuss:

$$\frac{1}{2} \frac{\sigma_{ij}^2}{C_{ij}} V \leq \sum_{k=1}^n (U_b + U_s + U_a)_k \quad (5)$$

$$\frac{1}{2} C_{ij} \varepsilon_{ij}^2 V \leq \sum_{k=1}^n (U_b + U_s + U_a)_k \quad (6)$$

where k accounts for individual substructures in the initial structure, and U_b , U_s , and U_a are respectively the bending, shear, and axial strain energies.

In the present problem, the difficulty is mainly due to the alternation of the two layers of fins forming the unit cell where the form of the cross-section depends on the position of the cut. To overcome this problem, the core is simplified and considered as a laminate composed of two repetitive alternating layers. Therefore, two new unit cells are considered each representing a layer, and the calculation is performed on each unit cell separately (Fig. 8-a). To simplify calculation, an equivalent structure is considered (Fig. 8-b) where fillets are replaced by straight lines.

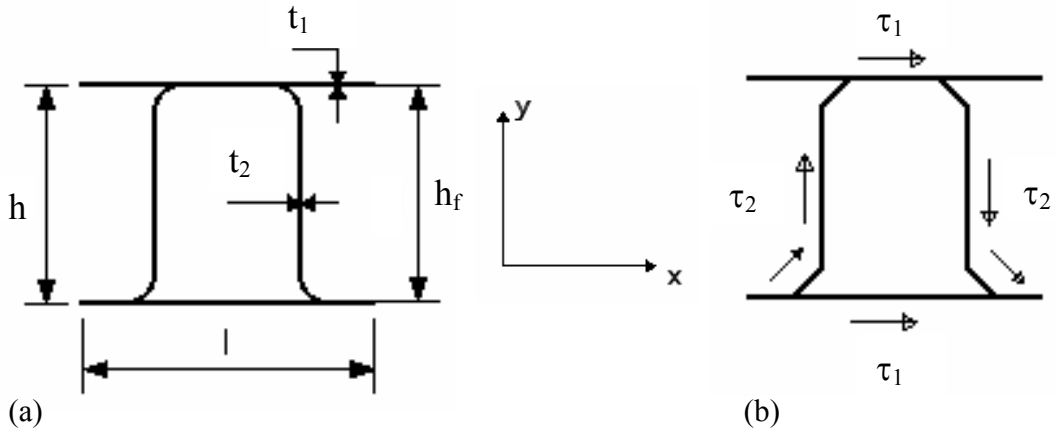


Fig. 8. (a) Unit cell representing a layer (b) Simplified unit cell

When a shear stress τ_{xz} is applied along the x-direction, the resulting apparent distributed shear flow is as shown in Fig. 8-b. The equilibrium equation and compatibility requirements are written as:

$$2t_2 \int_0^s \tau_2 \cos \vartheta ds + 2t_1 l \tau_1 = h l \tau_{xz} \quad (7)$$

$$2 \int_0^s \frac{\tau_2}{G} ds = \frac{\tau_2}{G} l \quad (8)$$

where G is the shear modulus of the constitutive material of the core, and θ is the angle between the fin and the x-axis (θ is constant in every portion of the fin), with

$$2 \int_0^s \cos \vartheta ds = l \quad (9)$$

Equations (7) and (8) lead to:

$$\tau_1 = \frac{2h \int_0^s ds}{lt_2 + 4t_1 \int_0^s ds} \tau_{xz} \quad (10)$$

and

$$\tau_2 = \frac{lh}{lt_2 + 4t_1 \int_0^s ds} \tau_{xz} \quad (11)$$

By applying equation (5), we obtain:

$$\frac{G_{xz}^e}{G} \geq \frac{lt_2}{2h \int_0^s ds} + \frac{2t_1}{h} \quad (12)$$

Similarly, applying a shear strain ε_{xz} and considering the corresponding compatibility conditions, equation (6) becomes:

$$lhG_{xz}^e \varepsilon_{xz}^2 \leq 2t_1 l G \varepsilon_{xz}^2 + 2t_2 G \varepsilon_{xz}^2 \int_0^s \cos^2 \theta ds \quad (13)$$

Simplifying equation (13), we obtain:

$$\frac{G_{xz}^e}{G} \leq \frac{2}{lh} \left(t_1 l + t_2 \int_0^s \cos^2 \theta ds \right) \quad (14)$$

Following a similar analysis process, the core shear modulus, G_{yz}^e , can be obtained as:

$$\frac{2t_2 h_f^2}{hl \int_0^s ds} G \leq G_{yz}^e \leq \frac{2t_2 \int_0^s \sin^2 \theta ds}{lh} G \quad (15)$$

4.2. Finite element calculation

Static behaviour of a unit cell has been evaluated via finite element numerical simulations. Two different structural configurations were considered: a “theoretical” geometry, similar to that used for analytical calculation and a “real” geometry, with initially distorted fins as observed in the real core structure. It should be emphasised that each fin layer has slightly different structural configuration and therefore a unique “real” geometry exhibiting the highest difference compared to the “theoretical” geometry has been arbitrarily chosen (Fig. 9).

The stiffness matrix was found by modelling the unit cell (constituted of a cold air fin and a hot air fin as in Fig. 6). Shell-type quadrangle elements were used. 1778 elements and 2007 nodes were necessary to model the unit cell. Six simulation cases were applied: 3 tractions and 3 shears. Boundary conditions for shear cases were inspired from Aitharaju and al. [13] as shown in Fig. 10-b. For tensile cases, calculations were performed with imposed loads on nodes belonging to elements defining the surface

perpendicular to the investigated axis (see Fig. 10-a). Symmetry conditions (1 translation, 2 rotations constrained) were imposed on side elements of the unit cell. In order to assess the validity of these boundary conditions, calculations were also performed on structures made of several unit cells gathered in all three directions as presented in Fig. 11. The tensile elastic moduli (obtained after equation (4)) were identical confirming the behaviour of a so modelled single unit cell is representative of the core behaviour. In order to compare finite element and analytical shear moduli results, calculations were also performed on cold air unit cell (see Fig. 9) and hot air unit cell separately.

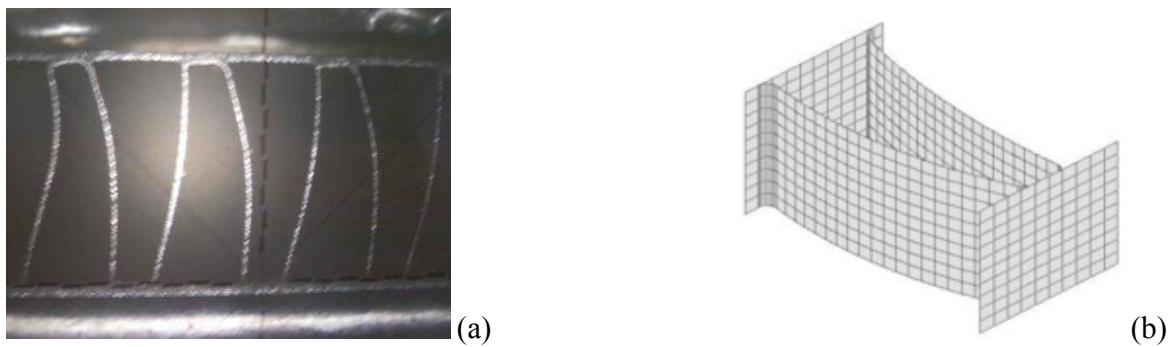


Fig. 9. Cold air fin (a) real structure, (b) finite element model with “real” geometry

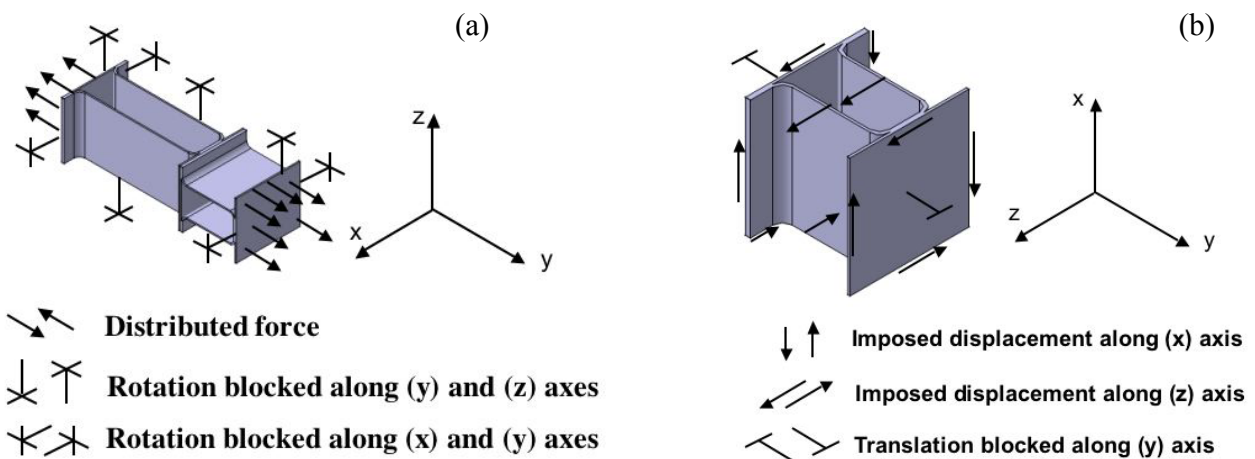


Fig. 10. Boundary conditions: (a) tensile case along (y) axis ; (b) shear case along (xz)

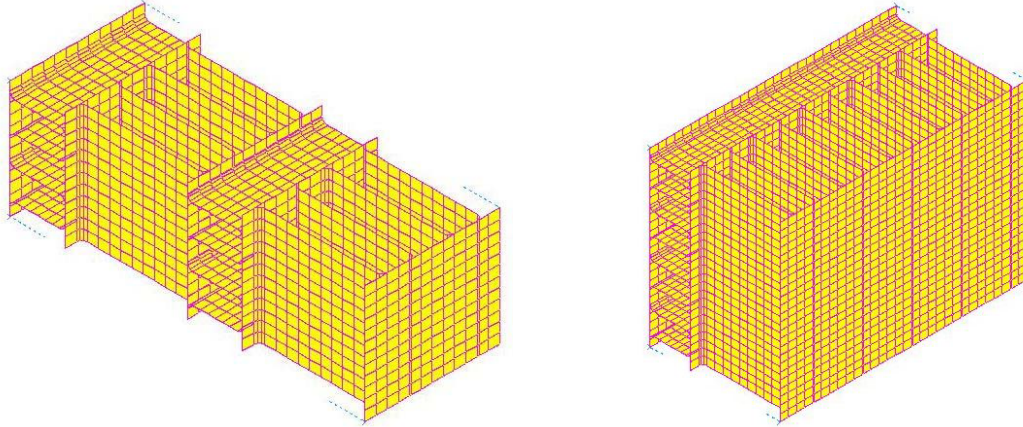


Fig. 11. Finite element models representing structures composed of different unit cells assembled along all three directions

4.3. Results and discussion

Table 1 presents the equivalent tensile elastic moduli obtained after analytical and numerical finite element analysis and the comparison with experimental tensile results. For finite element analysis, both “theoretical” and “real” unit cell elastic moduli are presented.

	Experimental	Analytical	FEM-T	FEM-R
E_x (GPa)		10.73	11.4	11.47
E_z (GPa)	13.54	13.47	13.24	13.97
E_y (GPa)	0.4	0.45	0.44	0.3

Table 1 : Comparison between equivalent elastic moduli obtained by tests, analytical calculation and finite element calculations on “theoretical” (FEM-T) and “real” geometry (FEM-R)

Along (z) and (x) directions, “theoretical” and “real” models provide the same elastic modulus. This is not surprising considering the assumption that along (x) and (z) directions, deformation of the unit cell is mainly due to the deformation of the plates and the longitudinal fins; the shape of the fins more or less bended along the (y) axis does not influence the tensile behaviour in the two other directions. Moreover the good agreement between experimental, analytical and finite element results confirms the reliability of this assumption. Along (y) direction, the variations between the different values are more important.

Analytical and finite element with “theoretical” structure modelling leads to similar elastic moduli which are higher than experimental one. This result suggests that the modelling is relevant in both approaches but that the so-obtained stiffness is over-estimated compared to the real structure. On the contrary the finite element analysis of “real” geometry gives a lower equivalent elastic modulus than experiments. This is due to the fact that, even if strictly copied from real fins, this selected shape is not more representative of the real global structure than the theoretical one: one must remind the structural configuration is not exactly the same from a layer to another in the whole sample. Subsequently, the experimental elastic modulus which is obtained by tensile tests on a sample constituted by several layers is an average value of elastic moduli from different layers probably ranging from 0.3 to 0.45 GPa. According to these results, it appears that modelling the static tensile behaviour along (y) axis is difficult. Unless completely modelling the whole core by finite elements, which presents only little interest, the “theoretical” solution remains reasonable with a variation from approximately 15% with the experimental values. As a conclusion, both analytical and numerical approaches based on « theoretical » unit cell are completely satisfactory to estimate the elastic moduli of the core. Moreover, these approaches have the advantage of adapting easily to other geometries of fins.

Concerning shear moduli, results are presented in Table 2. Due to their complexity for such structures, no shear tests were carried out. Consequently, only analytical and numerical results are available. Moreover, analytical analysis can only predict shear modulus along two directions for each layer. For these cases, finite element simulations with “theoretical” shape give satisfactory results within the range predicted by analytical calculations. However, the other results can not be validated properly. In addition, the shape of the unit cell seems to highly influence the shear behaviour perpendicular to (y) axis where the deformation is mainly located in the fins.

	G_{xy} (MPa)			G_{yz} (MPa)			G_{xz} (MPa)		
	Analytical	FEM-T	FEM-R	Analytical	FEM-T	FEM-R	Analytical	FEM-T	FEM-R
C-L		1.17	3.43	2650-3140	2840	1600	1.96-2.56	2.19	4.15
H-L	2560-3400	3400	2903		6.56	9.64	4.45-5.42	4.7	4.65
Unit Cell		0.77	5.9		10.7	31.04		3.06	3.01

Table 2 : Comparison between equivalent shear moduli obtained by analytical calculation and finite element calculations on “theoretical” (FEM-T) and “real” geometry (FEM-R) for cold air layer (C-L), hot air layer (H-L) and the unit cell.

5. Modelling of dynamic behaviour

5.1. Dynamic response of specimens

For dynamic behaviour, two models were considered: a) a homogenous model where samples are considered as a homogeneous structure with an equivalent stiffness matrix found by the above-mentioned static calculation and b) a laminated model where specimens are considered being formed by stacking alternatively two plates (cold air layer and hot air layer) each having equivalent orthotropic properties resulting from the above-mentioned static calculation. Fig. 12 presents both models for a sample similar to y-axis tensile test sample. Damping was not taken into account in calculation. A linear elastic dynamic calculation was performed and free vibration modes of specimens were computed. Equivalent densities were introduced based on samples real mass in order to take into account the weight of brazed joints. Samples were left free: all displacements and rotations were permitted. In addition, for the laminated model, static properties from both “theoretical” and “real” shape were used to perform dynamic calculations.

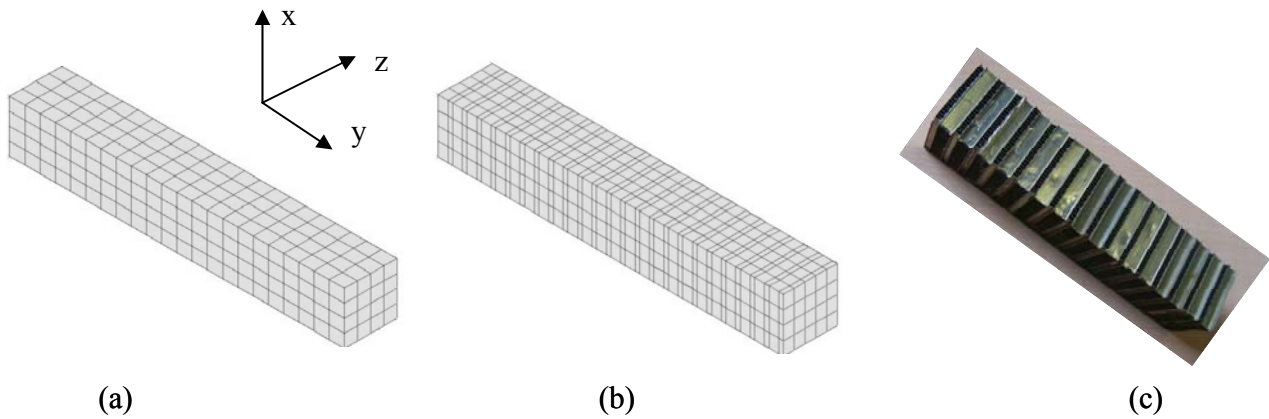


Fig. 12. y-axis dynamic samples: (a) homogenous model for dynamic simulation (b) laminated model for dynamic simulation, (c) test sample

5. 2. Results and discussion

As an example, experimental and numerical results are compared for two types of samples in Fig. 13. Mode shapes were not measured experimentally but for each set of numerical frequencies compared in Fig. 13, the mode shape was similar. Dynamic simulations with homogeneous model only gave consistent resonant frequencies values for y-axis sample; for z-axis samples, calculated natural frequency values are much lower than experimental ones. It is supposed that, for these two types of specimen, the difference between the shear behaviour of cold air and hot air layers is too important to be correctly represented by a model using an “average” behaviour. Therefore, this homogeneous model cannot be relevant enough for the dynamic behaviour of the samples. The laminate model exhibits good results compared to experimental frequencies. However, the model using static properties from “theoretical” shape (LM-T) is better than the model using static behaviour of “real” shape (LM-R). Variations between LM-T approach and experimental results are less than 4 and 10% for respectively y-axis and z-axis samples. For LM-R, variations range from 1 to 15% for y-axis specimen and are less than 10% for z-axis specimen. As a conclusion, it appears that, like for static analysis, numerical approach based on « theoretical » unit cell results provides a better and more relevant estimation of the global dynamic behaviour of the periodic structure constituting the heat exchanger core. Further

experiments and numerical simulations on the whole core are currently under progress to fully assess the validity and the reliability of the modelling.

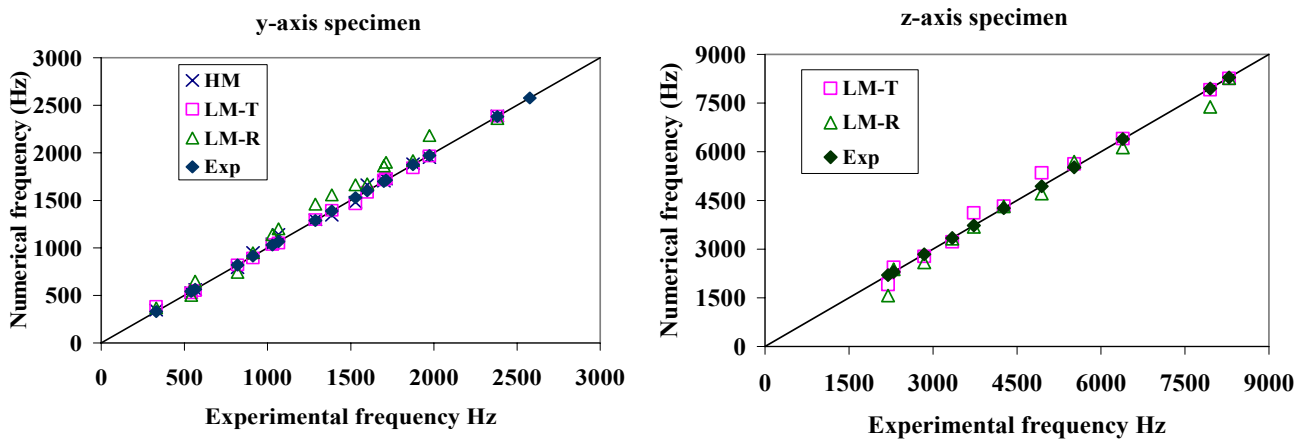


Fig. 13. Resonant frequencies for two types of specimen: comparison of experimental (Exp) and numerical results (HM: homogeneous model, LM-T: Laminate Model with static properties from “theoretical” shape, LM-R : Laminate Model with static properties from “real” shape)

6. Conclusion

Experimental, analytical and numerical approaches have been used to study and model the mechanical behaviour of an aircraft heat exchanger core consisting of a 3D-periodic structure. Concerning static characteristics, an approach based on the modelling of a unit cell (constituted of a cold air fin and a hot air fin) representative of the core behaviour has been proposed and validated. The core dynamic behaviour has been studied by means of finite element calculations and experimental tests. Two models have been evaluated: a) a homogeneous model where samples are considered being constituted of an homogeneous material with an equivalent stiffness matrix found by static calculation on a unit cell and b) laminated model where samples are considered being formed by stacking alternatively two plates (cold air layer and hot air layer) of two different materials each having equivalent orthotropic properties found by static calculations. Homogeneous model was found inadequate to reproduce experimental impulse-response results for all tested samples whereas laminated model has been validated. In addition, it has been shown that the use of a “theoretical” shape for determining static characteristics via a unit

cell is better than trying to reproduce the slight defects of the real fins. These approaches can further be used in the modelling of the whole exchanger and/or with a wider range of loading, including thermal loading. Moreover, it could be extended to other kind of heat exchanger with other fin geometries provided that it presents periodicity of the stacked layers.

References

1. Scida D, Aboura Z, Benzaggagh M.L, Bocherens E. A micromechanics model for 3D elasticity and failure of woven-fibre composite materials. *Composite Science and Technology* 1999;59:505-517.
2. Naik NK, Ganesh VK. An analytical method for plain weave fabric composites. *Composites* 1995;26:281-289.
3. Aboura Z, Talbi N, Allaoui S, Benzeggagh ML. Elastic behavior of corrugated cardboard: experiments and modelling. *Composite Structures* 2004;63:53-62.
4. Hohe J, Becker W. A refined analysis of the effective elasticity tensor for general cellular sandwich cores. *International Journal of Solids and Structures* 2001;38:3689-3717.
5. Davalos JF, Qiao P, Xu XF, Robinson J, Barth KE. Modeling and characterization of fiber-reinforced plastic honeycomb sandwich panels for highway bridge applications. *Composite Structures* 2001;52:441-452.
6. Kolpakova AG, Kalamkarov AL. Homogenized thermoelastic model for a beam of a periodic structure. *International Journal of Engineering Science* 1999;37:631-642.
7. Guinovart-Diaz R, Bravo-Castillero J, Rodriguez-Ramos R, Martinez-Rosado R, Serrania F, Navarrete M. Modeling of elastic transversely isotropic composite using the asymptotic homogenization method. Some comparisons with other models. *Materials Letters* 2002;56:889-894.
8. Ghosh S, Lee K, Moorthy S. Multiple scale analysis of heterogeneous elastic structures using homogenization theory and voronoi cell finite element method. *Int. J. Solids Structures* 1995;32(1):27-62.
9. Dib J, Bilteryst F, Batoz JL, Lewon I. Détermination par homogénéisation des propriétés mécaniques d'échangeurs de chaleur à plaques et ondes. 17^{ème} Congrès Français de Mécanique, Troyes, France, 2005.
10. Dib J, Bilteryst F, Batoz JL, Lewon I. Implementation of 3D homogenization techniques for the thermo-elastic FEM analysis of brazed plate-fin heat exchangers. In: Mota Soares CA et al. III European

Conference on Computational Mechanics Solids, Structures and Coupled Problems in Engineering, Lisbon, Portugal, 2006.

11. Grenestedt JL. Influence of wavy imperfections in cell walls on elastic stiffness of cellular solids. *J. Mech. Phys. Solids* 1998; 46(1): 29-50.

12. Ostoja-Starzewski M, Sheng PY, Alzebdeh K. Spring network models in elasticity and fracture of composites and polycrystals. *Computational Material Science* 1996;7:82-93.

13. Aitharaju VR, Averill RC. Three-dimensional properties of woven-fabric composites. *Composites Science and Technology* 1999;59:1901-1911.

Figure Captions

Fig. 1. A schematic presentation of the periodic structure of the heat exchanger core

Fig. 2 . Tensile test samples along (a) z-axis (b) y-axis

Fig. 3. Dynamic testing of specimen using IR technique

Fig. 4. Force-Deformation diagrams of tensile tests (a) z-axis (b) y-axis

Fig. 5. Example of a Fourier Transform of y-axis sample response

Fig. 6. Unit cell of the core

Fig. 7. Substructures and their corresponding analytical stiffness used for the estimation of the stiffness K_y of a unit cell

Fig. 8. (a) Unit cell representing a layer (b) Simplified unit cell

Fig. 9. Cold air fin (a) real structure, (b) finite element model with “real” geometry

Fig. 10. Boundary conditions: (a) tensile case along (y) axis ; (b) shear case along (xz)

Fig. 11. Finite element models representing structures composed of different unit cells assembled along all three directions

Fig. 12. y-axis dynamic samples: (a) homogenous model for dynamic simulation (b) laminated model for dynamic simulation, (c) test sample

Fig. 13. Resonant frequencies for two types of specimen: comparison of experimental (Exp) and numerical results (HM: homogeneous model, LM-T: Laminate Model with static properties from “theoretical” shape, LM-R : Laminate Model with static properties from “real” shape)

	Experimental	Analytical	FEM-T	FEM-R
Ex (GPa)		10.73	11.4	11.47
Ez (GPa)	13.54	13.47	13.24	13.97
Ey (GPa)	0.4	0.45	0.44	0.3

Table1 : Comparison between equivalent elastic moduli obtained by tests, analytical calculation and finite element calculations on “theoretical” (FEM-T) and “real” geometry (FEM-R)

	G_{xy} (MPa)			G_{yz} (MPa)			G_{xz} (MPa)		
	Analytical	FEM-T	FEM-R	Analytical	FEM-T	FEM-R	Analytical	FEM-T	FEM-R
C-L		1.17	3.43	2650- 3140	2840	1600	1.96-2.56	2.19	4.15
H-L	2560- 3400	3400	2903		6.56	9.64	4.45-5.42	4.7	4.65
Unit Cell		0.77	5.9		10.7	31.04		3.06	3.01

Table 2 : Comparison between equivalent shear moduli obtained by analytical calculation and finite element calculations on “theoretical” (FEM-T) and “real” geometry (FEM-R) for cold air layer (C-L), hot air layer (H-L) and the unit cell.